separations

MDPI

Article

Anti-Allergic and Antioxidant Potential of Polyphenol-Enriched Fractions from *Cyclopia subternata* (Honeybush) Produced by a Scalable Process

Carla Dippenaar [1,2], Hitoshi Shimbo [3], Kazunobu Okon [3], Neil Miller [1], Elizabeth Joubert [1,2], Tadashi Yoshida [3,*] and Dalene de Beer [1,2,*]

[1] Plant Bioactives Group, Post-Harvest & Agro-Processing Technologies Division, Agricultural Research Council, Stellenbosch 7599, South Africa
[2] Department of Food Science, Stellenbosch University, Stellenbosch 7602, South Africa
[3] Department of Applied Biological Science, Tokyo University of Agriculture and Technology, Tokyo 183-8509, Japan
* Correspondence: tyoshi@cc.tuat.ac.jp (T.Y.); dbeerd@arc.agric.za (D.d.B.)

Abstract: Anti-allergic activity was previously demonstrated for extracts of *Cyclopia subternata* Vogel plant material, containing substantial amounts of xanthones, benzophenones, dihydrochalcones, flavanones and flavones. Fractionation of a hot water extract on macroporous resin was performed aiming to increase its potency. Operating conditions for scaled-up fractionation of the extract were determined, using small-scale static and dynamic sorption/desorption experiments. The anti-allergic potential of the fractions was assessed based on inhibition of β-hexosaminidase release from IgE-sensitized RBL-2H3 cells. Given the role of oxidative stress in allergic reactions, the extract and fractions were also tested for their ability to scavenge the superoxide anion radical and inhibit xanthine oxidase (XO), an enzyme involved in its generation. The routine DPPH and ORAC assays were used for determination of the antioxidant capacity of the fractions. 3-β-D-Glucopyranosyl-4-*O*-β-D-glucopyranosyliriflophenone (IDG) had the lowest affinity for the resin, dictating selection of the optimal separation conditions. The extract was separated into four fractions on XAD1180N, using step-wise gradient elution with EtOH-water solutions. The major phenolic compounds present in the fractions were IDG and 3-β-D-glucopyranosyliriflophenone (fraction 1), mangiferin, isomangiferin, 3′,5′-di-β-D-glucopyranosyl-3-hydroxyphloretin and vicenin-2 (fraction 2), 3′,5′-di-β-D-glucopyranosylphloretin, eriocitrin and scolymoside (fraction 3) and hesperidin and *p*-coumaric acid (fraction 4). Fractionation was only partially effective in increasing activity compared to the extract, i.e., fractions 2, 3 and 4 in the DPPH• and XO assays, fractions 1 and 2 in the ORAC assay and fraction 1 in the β-hexosaminidase release assay. In vivo testing will be required to determine whether the increased activity of fractions is worth the effort and expense of fractionation.

Keywords: adsorption; anti-allergic activity; antioxidant activity; *Cyclopia subternata*; desorption; honeybush; macroporous resin chromatography

Citation: Dippenaar, C.; Shimbo, H.; Okon, K.; Miller, N.; Joubert, E.; Yoshida, T.; de Beer, D. Anti-Allergic and Antioxidant Potential of Polyphenol-Enriched Fractions from *Cyclopia subternata* (Honeybush) Produced by a Scalable Process. *Separations* **2022**, *9*, 278. https://doi.org/10.3390/separations9100278

Academic Editors: Norizan Ahmat and Juriyati Jalil

Received: 1 September 2022
Accepted: 19 September 2022
Published: 1 October 2022

1. Introduction

Over the past few decades, research elevated polyphenols from mostly unwanted food constituents to natural products with commercial value, due to a plethora of beneficial bioactivities. These include anti-allergic activities [1], which are very relevant, given the increase in the prevalence of food allergies [2] and other allergies such as asthma, especially in children [3]. Allergies not only negatively affect the quality of life, but they can also be fatal [3].

Polyphenols exert anti-allergic activity via many mechanisms [1,4]. Interaction with allergic effector cells such as mast cells can inhibit the release of mediators. As antioxidants, they may also limit the extent of cellular injury caused by free radicals during

the allergic insult [4]. Allergic reactions can be exacerbated by pro-inflammatory mediators such as reactive oxygen species (ROS) [5]. One of the endogenous sources of ROS is the xanthine/xanthine oxidase (XO) system, which forms the superoxide anion radical ($O_2^{\bullet-}$). Scavenging the radical and inhibiting XO would therefore help to alleviate oxidative stress [6]. Regular consumption of foods containing polyphenols may thus help to avoid or reduce allergic responses.

Cyclopia subternata Vogel (honeybush) is commonly consumed as a herbal tea and is a source of benzophenones, xanthones, dihydrochalcones, flavanones and flavones [7]. Hot water and 40% EtOH-water extracts of the plant material were found to induce regulatory T cells, implying that they would be effective against inflammation and allergy in vitro [8]. Interest in the potential of *C. subternata* extracts as functional food ingredients grew when it was found that the 40% EtOH-water extract also showed anti-allergic activity in mice [9]. The next step would be to enhance the bioactivity of the extract through polyphenol enrichment.

With eventual industrial production of a standardized product suitable for use as a food ingredient in mind, macroporous adsorbent resin chromatography (MARC) was selected to produce extract fractions enriched in specific compounds. MARC is not only relatively simple to operate but also does not require the use of toxic chemicals and it can be easily up-scaled [10]. Furthermore, non-toxic solvents such as water and EtOH are commonly used and regeneration of resins requires no heating, making the process both economically feasible and environmentally friendly [11].

This study aimed to develop an eco-friendly MARC protocol that would yield one or more fractions with higher anti-allergy potential than the hot water extract. Although the hot water extract of *C. subternata* was not tested in vivo [9], it is the obvious choice because it corresponds to the traditional preparation method of the herbal tea and is suitable as a food ingredient. Water is also the ultimate green solvent. Given that cell and animal studies are not appropriate for quality control in an industrial setting, we chose substitute assays that are suitable for routine analysis (faster and cheaper) and could potentially serve as proxies for "bioactivity" to evaluate the fractions. These include spectrophotometric assays for determining antioxidant capacity in general, as well as $O_2^{\bullet-}$ scavenging and XO inhibition. The widely used IgE-induced RBL-2H3 cell degranulation inhibitory assay [1,12] was used to determine the anti-allergy potential of the fractions compared to the extract.

2. Materials and Methods

2.1. Chemicals and Resins

Unless otherwise stated, all compounds were analytical-grade products from Sigma-Aldrich (St. Louis, MO, USA) or Merck (Darmstadt, Germany). Analytical grade ethanol (EtOH, ≥99.9%) was obtained from Servochem (Cape Town, South Africa). HPLC gradient-grade acetonitrile was supplied by Merck. Authentic reference standards, used for HPLC (purity > 95%), were obtained from Extrasynthese (Genay, France; eriocitrin), Karl Roth (Karlsruhe, Germany; luteolin), Phytolab (Vestenbergsgreuth, Germany; 3-β-D-glucopyranosyliriflophenone (IMG), mangiferin and vicenin-2) and Sigma-Aldrich (hesperidin, protocatechuic acid and *p*-coumaric acid). Minimal Essential Medium (MEM), penicillin and streptomycin were obtained from Gibco (New York, NY, USA). Tap water was purified to deionized water (Elix Advantage 5, Merck, Kenilworth, NJ, USA), which was further purified to HPLC grade water (Milli-Q Reference A plus, Merck).

Two food-grade polymeric adsorbents, namely Amberlite XAD 1180N and Diaion HP20 (Sigma-Aldrich), were rinsed with deionized water at a liquid: solid ratio of 6:1. Before each experiment, the moisture content of the resins was determined gravimetrically. A 2 g aliquot of resin was heated at 100 °C for 60 min using an HR73 Halogen Moisture Analyser (Mettler-Toledo, Greifensee, Switzerland).

2.2. Preparation of C. subternata Hot Water Extract

Shoots of *C. subternata* plants, harvested at two locations (Nietvoorbij research farm, Stellenbosch; Kanetberg, Barrydale, South Africa), were chopped into small pieces (≤3 mm), spread on drying trays and dried at 40 °C for 16 h in a cross-flow drying tunnel to ≤7% moisture content (wet basis). The dried plant material was pooled and milled using a Retsch mill (1 mm sieve; Retsch GmbH, Haan, Germany).

The milled plant material (ca. 120 g) was extracted with 1.2 L freshly-boiled deionized water in a pre-heated water bath at 93 °C for 30 min while swirling the mixture every 10 min. The warm extract was filtered through Whatman No. 4 filter paper and cooled to room temperature (23 °C). This process was repeated several times and the filtrates were pooled, frozen and freeze-dried (VirTis Advantage Plus, SP Scientific, Warminster, PA, USA). The freeze-dried extract was stored under desiccation.

2.3. Static Adsorption and Desorption

The freeze-dried *C. subternata* extract was reconstituted with deionized water. All experiments were performed in triplicate in polypropylene 24-well deep-well microplates (Axygen Scientific, Union City, CA, USA) according to the general procedure described by Miller et al. [13]. Briefly, except for the control wells, the wet resin (250 mg equivalent dry weight based on measured moisture content) was weighed into each well of the microplate. An aliquot (5 mL) of the reconstituted extract solution was then added to each well. The wells were sealed with aluminum film and the plate was shaken at 450 rpm (Eppendorf Mixmate, Hamburg, Germany) for different durations depending on the experiment. On completion of the treatment, the supernatant in each well was sampled and analyzed by HPLC with diode-array detection (DAD).

The effect of initial sample concentration on the adsorption of target compounds onto the resin was determined at room temperature (23 °C) for both XAD 1180N and HP20. This involved shaking of the resin and aqueous *C. subternata* extract solutions varying in concentration (1, 2, 3, 5, 7.5 and 10 mg/mL) for 24 h at room temperature. Control wells contained the extract solutions without resin. Subsequently, the effect of contact time on the adsorption of target compounds onto XAD 1180N was determined at room temperature, using an extract solution of 3 mg/mL. Separate wells of the microplate represented individual contact times (20, 40, 60, 90, 120 and 180 min). Control wells containing extract solutions without resin were prepared for each time point. The wells were sampled at the aforementioned time points from 0–180 min.

A range of EtOH-water concentrations (0, 5, 10, 15, 20, 30, 40, 50, 75, 100%; v/v) was investigated to determine an appropriate EtOH concentration for desorption of the target compounds from the loaded resin. A batch of loaded resin was prepared by mixing the aqueous *C. subternata* extract solution (3 mg/mL) and resin (5:1; v/v ratio) and shaking the mixture at room temperature for 90 min. After removal of the supernatant by vacuum filtration, portions of the loaded resin, equaling 250 mg of dry resin, were weighed into the wells of the microplate. Aliquots (5 mL) of the EtOH-water mixtures were added to the wells containing loaded resin and shaken for 4 h at room temperature. Control wells, without added resin, but with extract or the supernatant after resin loading were included for each EtOH concentration.

For each experiment, the adsorption capacity (Q_e; mg/g), adsorption ratio (AR, %) and/or desorption ratio (DR, %) were calculated as follows [14]:

$$Q_e = \frac{V_0(C_0 - C_e)}{W} \quad (1)$$

$$AR\ (\%) = \frac{V_0(C_0 - C_e)}{C_0 V_0} \times 100 \quad (2)$$

$$DR\ (\%) = \frac{C_d V_d}{V_0(C_0 - C_e)} \times 100 \quad (3)$$

where C_0 is the initial concentration of the target compound in solution (mg/mL); C_e is the equilibrium concentration of the target compound in solution (mg/mL); V_0 is the volume of extract solution added to the well (mL); W is the dry mass of the resin (g); C_d is the concentration of the target compound in the desorption solution at equilibrium (mg/mL); V_d is the volume of the desorption solution (mL).

2.4. Small-Column Dynamic Adsorption and Desorption

A glass column wet-packed with XAD 1180N macroporous resin (Omnifit Labware, Diba Industries Inc., Danbury, CT, USA; ID 25 mm, height 700 mm, resin bed height 195 mm, bed volume (BV) 960 mL) was used for small-scale dynamic adsorption and desorption experiments. A Gilson Minipuls 3 peristaltic pump (Gilson Inc., Middleton, WI, USA) was fitted at the bottom of the column to control the eluent flow rate by suction. The bed height-to-diameter ratio was 7.8:1. Before sample loading, the column was conditioned by flushing it with six BVs of deionized water. All dynamic sorption experiments were performed in triplicate at room temperature (23 °C).

To determine the breakthrough volume, 10 BVs of aqueous *C. subternata* extract solution (10 mg/mL) were loaded onto the column at a flow rate of 2 BV/h. Each BV of eluate (n = 10) was collected and analyzed by HPLC-DAD. Thereafter, a dynamic desorption assay was performed. Seven BVs of aqueous *C. subternata* extract solution (10 mg/mL) were loaded onto the column, followed by step-wise gradient elution using 3 BVs each of 12, 20, 30 and 50% EtOH at a flow rate of 2 BV/h. The successive BVs of eluate were collected and analyzed by HPLC-DAD.

2.5. Large-Column Fractionation

Fractionation of the aqueous *C. subternata* extract solution was performed on a larger scale to produce four fractions enriched in different phenolic compounds. The protocol described in Section 2.4 was up-scaled by a factor of 22 while maintaining a bed height-to-diameter ratio of 7.8:1. Fractionation was carried out in a 70-mm internal diameter glass column. A peristaltic pump (Model 505U, Watson-Marlow Ltd., Falmouth, England) fitted to the bottom of the column was used to control the eluate flow rate (2 BV/h). The column was wet-packed with resin up to a bed height of 550 mm, equivalent to a BV of 2.1 L. Following column loading with 7 BVs of the extract solution (10 mg/mL; total mass loaded = 147 g), step-wise gradient elution was performed using 12, 20, 30 and 50% aqueous EtOH (3 BVs each). Each BV of the eluate was collected separately and analyzed by HPLC-DAD, whereafter they were pooled according to phenolic composition to produce four fractions: fraction 1 (12% EtOH BV 1 and 2), fraction 2 (12% EtOH BV 3 and 20% EtOH BV 1, 2 and 3), fraction 3 (30% EtOH BV 1, 2 and 3) and fraction 4 (50% EtOH BV 1, 2 and 3). The EtOH was removed by vacuum rotary evaporation at 40 °C (Rotavapor R-215, Buchi, Flawil, Switzerland). The aqueous residue was freeze-dried and analyzed using HPLC-DAD. The freeze-dried fractions were stored in screw cap glass jars sealed with Parafilm under desiccation.

2.6. Identification and Quantification of Phenolic Compounds

The phenolic composition of the samples was determined using a validated HPLC-DAD method developed for *C. subternata* [7]. Separation was achieved on an Agilent 1200 series HPLC system (Agilent Technologies Inc., Santa Clara, CA, USA). Residual EtOH in samples from the desorption experiments was removed by evaporation under vacuum at 45 °C for 2 h (Savant SPD2010 SpeedVac Concentrator, Thermo Scientific, Waltham, MA, USA). For analysis, these samples and the freeze-dried samples were dissolved in water or 10% dimethyl sulfoxide (DMSO). Ascorbic acid (ca. 10 mg/mL final concentration) was added to the samples and the mixtures were filtered through 0.45 µm pore-size Millex-HV syringe filters (Merck). Eight-point calibration curves of the available reference standards were set up for the quantification of the compounds. Due to the lack or scarcity of authentic reference standards, isomangiferin, scolymoside, 3-β-D-glucopyranosyl-4-*O*-β-

D-glucopyranosyliriflophenone (IDG), 3-β-D-glucopyranosylmaclurin (MMG), 3′,5′-di-β-D-glucopyranosylphloretin (PDG) and 3′,5′-di-β-D-glucopyranosyl-3-hydroxyphloretin (HPDG) were quantified based on their response factors (ratio of slopes for compound and reference compound) relative to mangiferin, luteolin, hesperidin, vicenin-2, hesperidin and hesperidin, respectively. Eriocitrin, hesperidin, protocatechuic acid, IDG, IMG, PDG and HPDG were quantified at 288 nm, and MMG, mangiferin, isomangiferin, vicenin-2, *p*-coumaric acid, scolymoside and luteolin at 320 nm.

Compound identity and peak purity were confirmed using high-resolution-mass spectrometry (HR-MS). The same HPLC method was used for separation as for quantification using a Waters Acquity UPLC and a Synapt G2 Q-ToF mass spectrometer (Waters, Milford, MA, USA). The electrospray ionization (ESI) source operated in negative ionization mode. A sodium formate solution was used for mass calibration and leucine enkephalin served as the lock spray solution. The eluent was split in a 1:1 ratio before entering the ionization chamber. MassLynx v.4.1 (Waters) software was used for data acquisition and analysis. A mass range of 150 to 1500 amu was scanned. Other MS parameters were: capillary voltage, −2.5 kV; sampling cone voltage, 15 V; source temperature, 120 °C; desolvation temperature, 275 °C; desolvation nitrogen (N_2) gas flow, 650 L/h; cone gas flow (N_2), 50 L/h. MS^E was performed by ramping the trap collision energy from 20.0 to 60.0 V.

2.7. Radical Scavenging Assays

2.7.1. Superoxide Anion Radical ($O_2^{\bullet -}$) Scavenging Assay

The $O_2^{\bullet -}$ scavenging activity of the extract and fractions (prepared in 10% DMSO) was determined using a method adapted from Chisté et al. [15]. The scavenging activity of the samples was determined spectrophotometrically in 96-well, flat-bottom microplates (Greiner Bio-One, Kremsmünster, Austria) using a BioTek SynergyHT microplate reader (BioTek Instruments, Winooski, VT, USA). The half-maximal inhibitory concentration (IC_{50}) of a sample was determined, using a 12-point concentration range. The analysis was done in triplicate and the assay was repeated three times to obtain triplicate IC_{50} values.

Potassium phosphate buffer (100 mM; pH 7.4) was used to prepare the reagents (phenazine methosulphate [PMS], nicotinamide adenine dinucleotide [NADH] and nitro blue tetrazolium [NBT]). The reaction mixture containing equal volumes (60 µL) of 664 µM NADH, 1 mM NBT and the sample was incubated at 37 °C for 2 min. Control wells contained 10% DMSO instead of the sample. Then, 60 µL of 108 µM PMS was dispensed into each of the control and sample wells (final reaction volume = 240 µL). Each sample well had a corresponding blank well, containing 60 µL buffer instead of PMS. Absorbance at 560 nm was measured at 0 and 2 min for all wells. The $O_2^{\bullet -}$ scavenging activity of the samples was calculated as follows:

$$\text{Activity } (\%) = \left(1 - \frac{A_S - A_B}{A_C}\right) \times 100 \quad (4)$$

where A_S, A_B and A_C refer to the net absorbance (difference in absorbance measured at 2 and 0 min) of the sample, blank and control, respectively.

2.7.2. 2,2-Diphenyl-1-picrylhydrazyl Radical ($DPPH^{\bullet}$) Scavenging Assay

The $DPPH^{\bullet}$ scavenging activity of the extract and fractions (prepared in 10% DMSO) was determined in 96-well microplate format [16] using a BioTek SynergyHT microplate reader (BioTek Instruments), and a 12-point concentration range of each sample was used for the determination of its IC_{50} value. All sample concentrations were analyzed in triplicate and the assay was repeated three times to determine triplicate IC_{50} values.

2.7.3. Oxygen Radical Absorbance Capacity Assay (ORAC)

The ORAC values of the extract and fractions (prepared in 10% DMSO) were determined in triplicate according to the method of Huang et al. [17]. Fluorescence was

measured using a BioTek SynergyHT microplate reader. The total antioxidant capacity (TAC_{ORAC}) of the extract and fractions was expressed in µmoles Trolox equivalents/g.

2.8. Xanthine Oxidase (XO) Inhibition Assay

Inhibition of XO by the extract and fractions (prepared in 10% DMSO) was determined in triplicate at three concentrations according to a method adapted from Leiro et al. [18]. Absorbance measurements of the samples were determined using 96-well, flat-bottom microplates (Greiner Bio-One) and a BioTek SynergyHT microplate reader. The reaction mixture consisted of equal volumes (60 µL) of 1 mM EDTA disodium salt dihydrate in 100 mM potassium phosphate buffer (pH 7.4), XO solution (0.025 U/mL) and sample or allopurinol (positive control; 1.36 µg/mL in 10% DMSO) or 10% DMSO (negative control). The microplate was incubated at 37 °C for 3 min, whereafter the reaction was initiated by adding 60 µL of 4 mM xanthine to each of the negative control, sample and allopurinol wells (final reaction volume = 240 µL). Each sample well and allopurinol well had a corresponding blank well containing 60 µL buffer instead of the xanthine solution. Absorbance measurements at 295 nm were recorded every 30 s for 8 min. The XO inhibition activity of the test samples and allopurinol was calculated as follows:

$$\text{XO inhibition } (\%) = \left(1 - \frac{A_s - A_{SB}}{A_C}\right) \times 100 \quad (5)$$

where A_S, A_{SB} and A_C refer to the net absorbance (difference in absorbance measured at 8 and 0 min) of the sample, sample blank and negative control, respectively.

2.9. β-Hexosaminidase Release Assay (Anti-Allergy Potential)

RBL-2H3 cells, purchased from JCRB (Osaka, Japan), were cultured in 96-well plates (Corning, NY, USA) at 5×10^4 cells/well using Minimal Essential Medium (MEM) supplemented with 100 U/mL of penicillin, 100 µg/mL of streptomycin and 10% fetal bovine serum. Anti-DNP-IgE antibody (Sigma) was added to the wells at 500 ng/mL. After culturing for 24 h, the medium was removed and the cells were washed twice with MEM. The samples dissolved in MEM were added at specific concentrations (62.5, 125 and 250 µg/mL); wortmannin (positive control) was added at 100 nM. MEM was added to the blank wells. After incubation for 30 min, 2,4-dinitrophenyl-human serum albumin was added to all wells at 5 ng/mL. After 1 h of incubation, the supernatants were collected from the wells and the lysis buffer (1% Triton X-100 in 50 mM Tris and 20 mM EDTA; pH 7.5) was added to each well. The plates were sonicated, and the cell lysates were collected from the wells. The same procedure was carried out for the wells without samples and cells to serve as cell lysate blank. The β-hexosaminidase activity of each supernatant and cell lysate was measured as follows: The same volume of substrate solution (1.3 mg/mL of 4-nitrophenyl-*N*-acetyl-β-D-glucosaminide in 0.1 M citrate buffer) was added to each supernatant and lysate, and stop solution (0.1 M Na_2CO_3 + 0.1 M $NaHCO_3$) was added after incubating for 90 min. The absorbance of each sample was measured at 405 nm. The release rate was calculated as follows:

$$\text{Release rate } (\%) = 100 \times \left[\frac{A_S - A_{SB}}{(A_s - A_{SB}) + (A_L - A_{BL})}\right] \quad (6)$$

where A_S, A_{SB}, A_L and A_{BL} refer to the absorbance of the sample, sample blank, cell lysate and cell lysate blank, respectively.

2.10. Data Analysis

Univariate analysis of variance (ANOVA), using the General Linear Models procedure (SAS Version 9.4; SAS Institute Inc., Cary, NC, USA), was performed to compare treatments for the data obtained from the static sorption tests. Fisher's least significant difference

was determined at the 5% level to compare treatment means where significant differences ($p < 0.05$) were found.

The half-maximal inhibitory concentration (IC_{50}) for $O_2^{\bullet -}$ and $DPPH^{\bullet}$ scavenging activity was determined by non-linear regression analysis of the concentration-effect data (log concentration vs. % scavenging) using GraphPad Prism (Version 8.2.1; GraphPad Software, San Diego, CA, USA). The four-parameter variable slope regression model was used, with the bottom value for % scavenging constrained to a constant value of 0. Triplicate IC_{50}, TAC_{ORAC} and XO inhibition values were also subjected to ANOVA to compare the values for the extract and fractions.

The statistical analysis of the β-hexosaminidase release assay data was performed by one-way ANOVA followed by the Dunnett test with $p < 0.05$ considered significant.

3. Results

3.1. Optimization of MARC Parameters

Static sorption assays were performed to determine the optimal sample concentration, adsorption time and desorption solvent for the separation of the target compounds.

The sample concentration affected the adsorption capacities (Table S1) and ARs (Table S2) of the phenolic compounds to the resins. At the highest sample concentration, XAD 1180N had a significantly higher ($p < 0.05$) adsorption capacity for IDG, IMG, HPDG, isomangiferin, vicenin-2 and *p*-coumaric acid than HP20. However, at this concentration, HP20 had a significantly higher ($p < 0.05$) adsorption capacity for PDG, eriocitrin, hesperidin, mangiferin and scolymoside than XAD 1180N. Even at the highest sample concentration, the flavanones (eriocitrin and hesperidin), dihydrochalcones (PDG and HPDG) and flavones (scolymoside and vicenin-2) had ARs of 100% for both resins (data not shown). Mangiferin and isomangiferin had ARs > 95%, irrespective of loading concentration and resin. The AR for IDG was the limiting factor as it decreased from 88.5% to 72.2% and 87.6% to 62.5% for XAD 1180N and HP20, respectively, when the sample concentration was increased from 1 to 10 mg/mL. For adequate adsorption of all the target compounds onto the macroporous resin, 3 mg/mL was selected. Furthermore, the XAD 1180N resin was selected for further experiments due to its higher ARs compared with that of HP20. Many of the compounds reached maximum adsorption at 20 min, whereas some increased their adsorption marginally up to 60 min (Figure S1). To ensure maximum adsorption of all compounds, 90 min was selected.

EtOH concentration affected the desorption of the compounds, resulting in large variations in the DR of a compound (Figure 1). IDG, *p*-coumaric acid and IMG already started to desorb in pure water (0% EtOH) with DRs equaling 14.9, 6.9 and 4.9%, respectively. On the other hand, mangiferin and isomangiferin had extremely low DR values ($\leq$1%) and none of the dihydrochalcones, flavanones and flavones was detected in the supernatant. Except for hesperidin and *p*-coumaric acid, all compounds reached 50% desorption at 20–30% EtOH. For these two compounds, an EtOH concentration > 30% was necessary to achieve 50% desorption. Hesperidin was completely desorbed at 75% EtOH.

Small-column dynamic experiments were conducted at a flow rate of 2 BV/h to determine the final protocol before up-scaling of the separation. Initial experiments using 15 BVs of aqueous *C. subternata* extract solution (3 mg/mL) showed breakthrough of IDG after loading 12 BVs of the extract solution (data not shown). The sample concentration was, therefore, increased to 10 mg/mL to reduce the breakthrough volume, as well as the time required to load the column. The breakthrough point was set at 10% to ensure minimal loss of IDG.

Breakthrough curves for IDG and IMG (Figure 2) show a gradual increase in the leakage of IDG and IMG from the column as the loading volume increased to seven BVs. Further loading of the column resulted in a rapid increase in the IDG concentration in the eluent, surpassing the 10% breakthrough set point; therefore, 7 BVs (672 mL; 6.72 g extract) were determined as the maximum sample loading volume of the column.

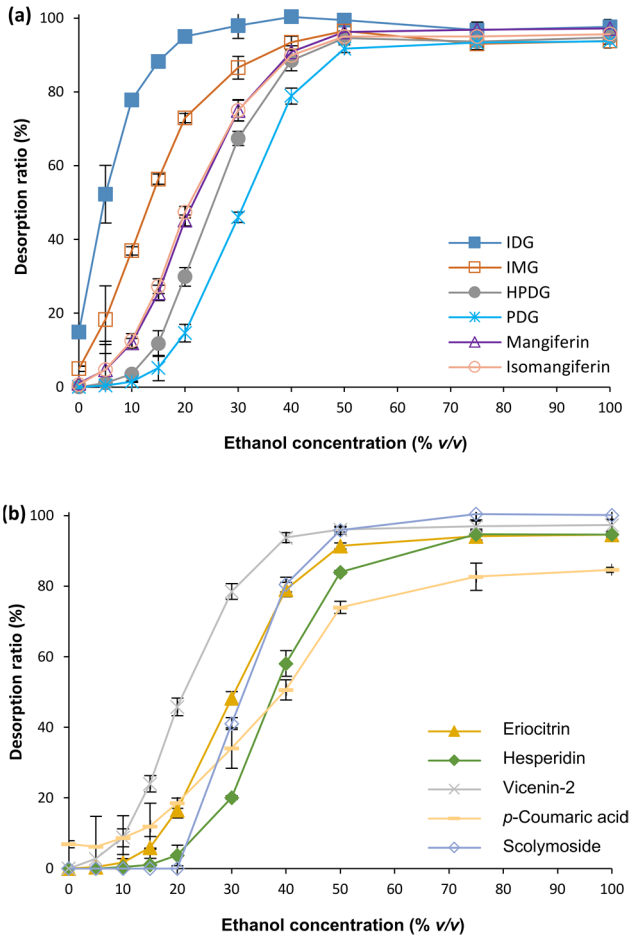

Figure 1. Desorption ratios of *Cyclopia subternata* benzophenones, dihydrochalcones and xanthones (**a**) and flavanones, flavones and a phenolic acid (**b**) on XAD 1180N macroporous resin as a function of ethanol concentration (% *v*/*v*), using static desorption. Data are given as mean ± standard deviation (n = 3). Abbreviations: IDG, 3-β-D-glucopyranosyl-4-*O*-β-D-glucopyranosyliriflophenone; IMG, 3-β-d-glucopyranosyliriflophenone; HPDG, 3′,5′-di-β-D-glucopyranosyl-3-hydroxyphloretin; PDG, 3′,5′-di-β-D-glucopyranosylphloretin.

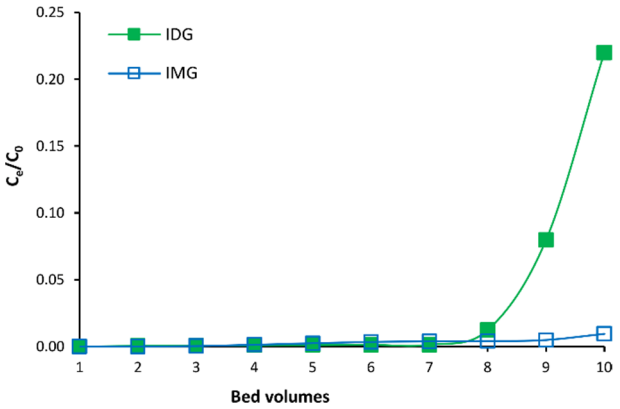

Figure 2. Dynamic breakthrough curves of *Cyclopia subternata* phenolic compounds on XAD 1180N macroporous resin at 2 BV/h in the small-scale column. Abbreviations: IDG, 3-β-D-glucopyranosyl-4-*O*-β-D-glucopyranosyliriflophenone; IMG, 3-β-D-glucopyranosyliriflophenone.

A step-wise solvent gradient consisting of 12, 20, 30 and 50% aqueous EtOH (3 BVs of each) was employed for the dynamic desorption of the target compounds from the loaded

resin column at a flow rate of 2 BV/h. Complete desorption of IDG was achieved after 2 BVs of 12% EtOH (Figure 3). Most of the IMG (64.1%) also eluted after 2 BVs of 12% EtOH, with the remaining IMG eluting in the third BV of 12% EtOH. Desorption of mangiferin, isomangiferin and vicenin-2 occurred gradually with successive BVs of 12% EtOH and the addition of 1 BV of 20% EtOH resulted in desorption maxima for mangiferin, isomangiferin and vicenin-2. Maximum desorption of HPDG occurred at 2 BVs of 20% EtOH, along with the co-elution of PDG, scolymoside and eriocitrin. A sharp increase in the desorption of PDG, scolymoside, eriocitrin and hesperidin was observed with successive BVs of 30% EtOH. Hesperidin, accompanied by the co-elution of small quantities of PDG, *p*-coumaric acid and scolymoside, was completely desorbed after 3 BVs of 50% EtOH.

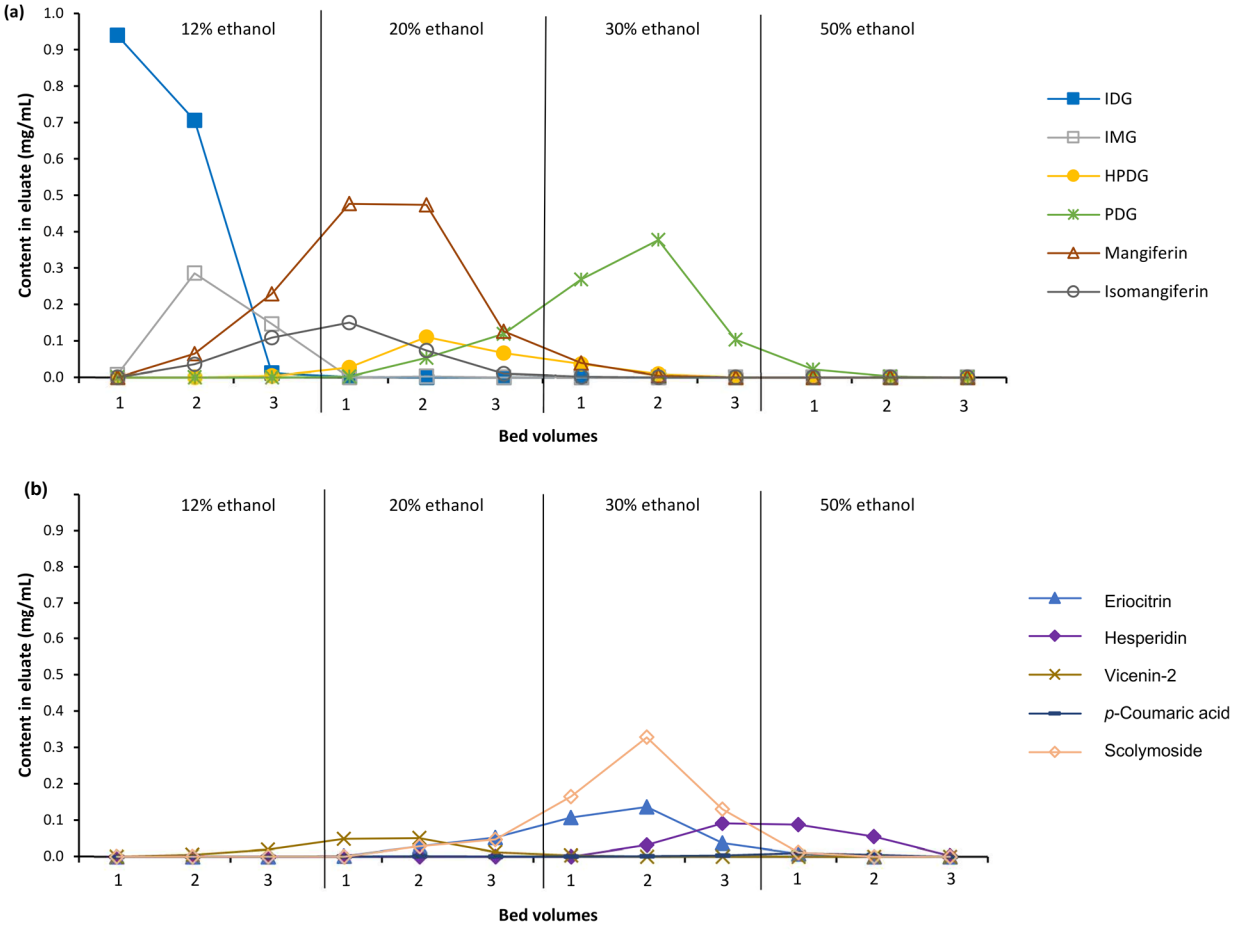

Figure 3. Dynamic desorption curves of *Cyclopia subternata* benzophenones, dihydrochalcones and xanthones (**a**) and flavanones, flavones and a phenolic acid (**b**) using different concentrations of ethanol solutions in the small-scale column. Abbreviations: IDG, 3-β-D-glucopyranosyl-4-*O*-β-D-glucopyranosyliriflophenone; IMG, 3-β-D-glucopyranosyliriflophenone; HPDG, 3′,5′-di-β-D-glucopyranosyl-3-hydroxyphloretin; PDG, 3′,5′-di-β-D-glucopyranosylphloretin.

3.2. Fractionation of C. subternata Extract Using MARC

The small-scale separation was scaled-up 22-fold by keeping the bed height-to-column diameter constant. To obtain four fractions enriched in different phenolic compounds, fractions were pooled based on the data from the dynamic desorption curves (Figure 3). Content values of the compounds for the extract and fractions are summarized in Table 1. The HPLC-DAD chromatograms are depicted in Supplementary information (Figure S2). LC-HR-MS data are provided in Table S3. Of the 147 g of extract loaded onto the resin column, a total of 97.8 g was recovered. The recovery of the individual phenolic compounds varied from 67.7% (hesperidin) to 100% (isomangiferin) (average 87.7%).

Table 1. Phenolic content (g/100 g) of a green *Cyclopia subternata* hot water extract and four fractions (including enrichment factors [a] in brackets), from large-scale fractionation on XAD 1180N.

Compound	Extract	Fraction 1	Fraction 2	Fraction 3	Fraction 4	Recovery Yield (%)
IDG	2.128	15.68 (7.4)	0.180 (0.1)	0.028 (0.01)	nd	94.9
IMG	0.702	2.555 (3.6)	1.494 (2.1)	0.024 (0.03)	nd	86.9
Mangiferin	1.921	1.403 (0.7)	8.594 (4.5)	0.417 (0.2)	0.016 (0.01)	99.2
Isomangiferin	0.507	0.545 (1.1)	2.328 (4.6)	0.027 (0.1)	nd	100
HPDG	0.388	0.050 (0.1)	1.386 (3.6)	0.228 (0.6)	nd	84.3
PDG	1.305	nd	1.697 (1.3)	2.546 (2.0)	0.333 (0.3)	78.2
Eriocitrin	0.464	nd	0.737 (1.6)	0.931 (2.0)	0.123 (0.3)	85.2
Hesperidin	1.130	nd	nd	1.069 (0.9)	5.950 (5.3)	67.7
Vicenin-2	0.231	0.151 (0.7)	1.045 (4.5)	0.047 (0.2)	nd	98.7
Scolymoside	0.977	nd	0.998 (1.0)	2.021 (2.1)	0.558 (0.6)	78.6
p-Coumaric acid	0.031	nd	0.019 (0.6)	0.030 (1.0)	0.151 (4.8)	75.9
Yield (g and percentage of extract)		18.7 (12.6%)	27.9 (18.8%)	39.2 (26.5%)	12.0 (8.1%)	

[a] Enrichment factors < 1 indicate depletion, while enrichment factors between 1 and 2 indicate minimal enrichment. Abbreviations: HPDG, 3′,5′-di-β-D-glucopyranosyl-3-hydroxyphloretin; IDG, 3-β-D-glucopyranosyl-4-*O*-β-D-glucopyranosyliriflophenone; IMG, 3-β-D-glucopyranosyliriflophenone; nd = not detected; PDG, 3′,5′-di-β-D-glucopyranosylphloretin.

Fraction 1 was enriched 7.4- and 3.6-fold with IDG and IMG, respectively, compared with the extract (Table 1). Small amounts of HPDG, mangiferin, isomangiferin and vicenin-2 were also present along with trace quantities of the minor benzophenone, MMG, two tetrahydroxyxanthone-di-*O*,*C*-hexose isomers, two phenolic acid glycosides and an eriodictyol-*O*-(hexose-*O*-deoxyhexose) as detected by MS (Table S3). The main compounds in fraction 2 were mangiferin and isomangiferin. Their content and that of HPDG and vicenin-2 were increased 4.5-, 4.6-, 3.6- and 4.5-fold, respectively. All the other major compounds, except hesperidin, were also present in fraction 2, but in smaller quantities than the xanthones. MS analysis of fraction 2 showed trace quantities of MMG, a tetrahydroxyxanthone-di-*O*,*C*-hexose, a phenolic acid glycoside and a pentahydroxyxanthone-*C*-hexose. Eriocitrin, PDG and scolymoside were increased by two-fold in fraction 3. In addition to these compounds, fraction 3 contained all the major compounds and traces of two pentahydroxyxanthone-*C*-hexose isomers, an eriodictyol-*O*-hexose and isorhoifolin. Fraction 4 consisted predominantly of hesperidin (5.3-fold enrichment) together with small amounts of eriocitrin, PDG, mangiferin, *p*-coumaric acid and scolymoside and traces of a naringenin glycoside and isorhoifolin.

3.3. Bioactivity of C. subternata Extract and Fractions

The radical scavenging activity of the extract and fractions was evaluated using three assays, i.e., the $O_2^{\bullet -}$ scavenging, DPPH$^\bullet$ scavenging and ORAC assays (Table 2). The samples scavenged $O_2^{\bullet -}$ in the descending order of activity: fraction 3 ≈ fraction 2 ≈ extract > fraction 4 > fraction 1. Considering scavenging of DPPH$^\bullet$, fractions 2, 3 and 4 were more effective ($p < 0.05$) than the extract with the IC_{50} value of fraction 2 (most effective) ca. 1.7-fold lower than that of the extract. In the ORAC assay, fractions 1 and 2 were the most effective as antioxidants with TAC_{ORAC} values significantly higher ($p < 0.05$) than that of the extract.

The extract and fractions showed relatively poor XO inhibitory activity (Figure 4) even at 400 µg/mL with their inhibitory activity varying in descending order: fraction 4 (33.8%) > fraction 2 (25.2%) ≈ fraction 3 (24.9%) > fraction 1 (15.7%) ≈ extract (15.0%). All samples were less potent than the positive control allopurinol, which inhibited 52.5% of the XO activity at a concentration of 1.36 µg/mL.

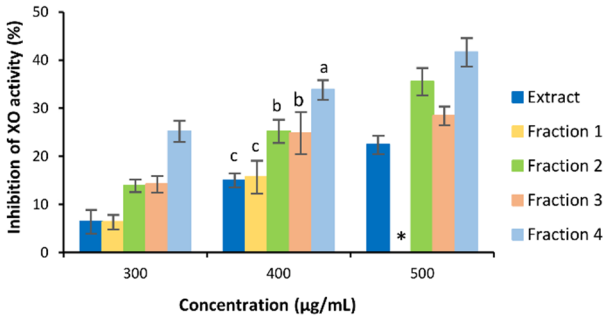

Figure 4. Xanthine oxidase (XO) inhibitory activity of a green *Cyclopia subternata* hot water extract and four fractions from large-scale fractionation on XAD 1180N as a function of sample concentration. Data are given as mean ± standard deviation (n = 3). Different letters above bars indicate significant differences ($p < 0.05$) at 400 µg/mL. * Value not available due to background absorbance of the fraction at this concentration.

Only the extract ($p < 0.05$) and fraction 1 ($p < 0.01$) were effective to inhibit mast cell degranulation as indicated by the decrease in the release of β-hexosaminidase in the RBL-2H3 cell model (Figure 5). Fraction 1 dose-dependently inhibited β-hexosaminidase release, but the extract was only significantly effective ($p < 0.05$) at 250 µg/mL.

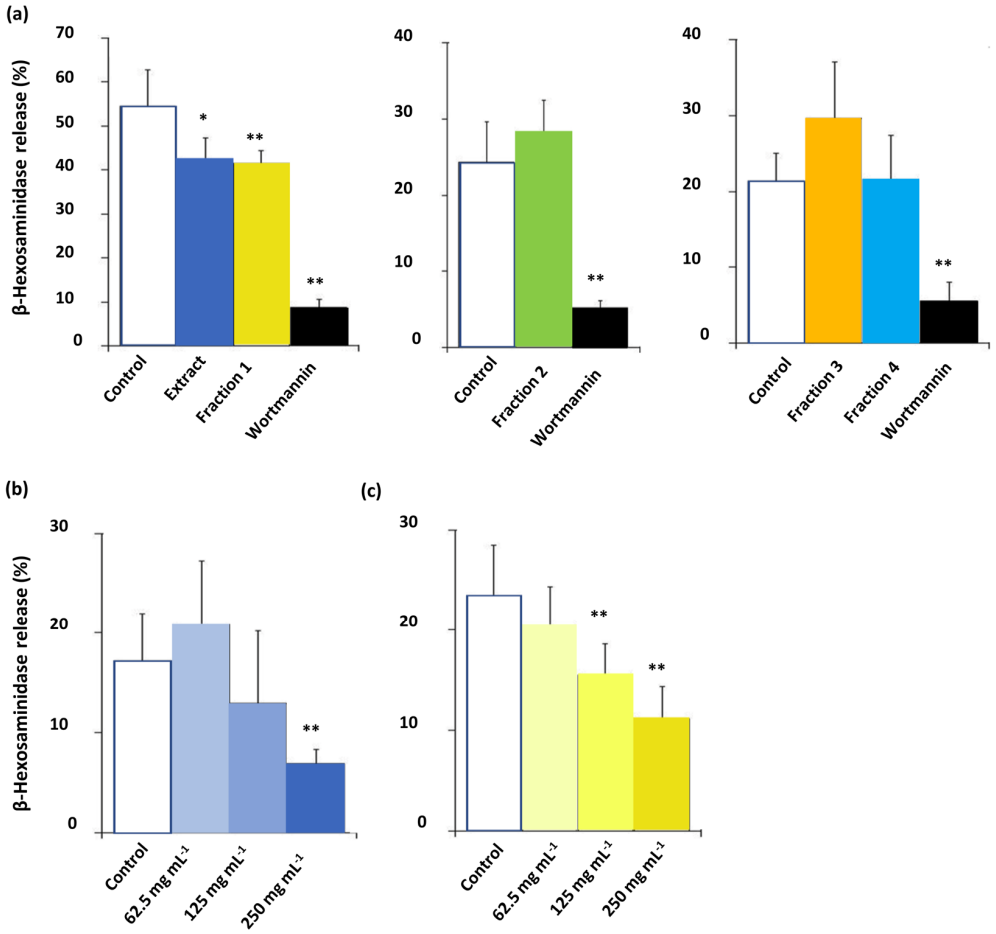

Figure 5. β-Hexosaminidase release inhibitory activity of (**a**) a green *Cyclopia subternata* hot water extract and four fractions from large-scale fractionation on XAD 1180N at 250 µg/mL and (**b**) the extract and (**c**) fraction 1 at three concentrations (62.5, 125 and 250 µg/mL). * and ** indicate significant differences versus the control at $p < 0.05$ and $p < 0.01$, respectively.

Table 2. Antioxidant activity of a green *Cyclopia subternata* hot water extract and fractions obtained from large-scale fractionation on XAD 1180N.

Sample	IC_{50} (SOA) [a]	IC_{50} (DPPH) [b]	TAC_{ORAC} [c]
Extract	141c ± 5	13.7b ± 0.4	2877b ± 167
Fraction 1	305a ± 14	19.3a ± 1.0	4237a ± 1
Fraction 2	119c ± 4	8.28e ± 0.28	4224a ± 965
Fraction 3	115c ± 19	10.2d ± 0.4	2740b ± 105
Fraction 4	182b ± 26	12.1c ± 1.3	3199ab ± 434

[a] Half-maximal inhibitory concentration (IC_{50}) against superoxide anion radical (µg/mL); [b] half-maximal inhibitory concentration against DPPH radical (µg/mL); [c] average total antioxidant capacity values expressed as µmoles Trolox equivalents/g. Data are given as mean ± standard deviation. Different letters in the same column indicate significant differences ($p < 0.05$).

4. Discussion

4.1. Production of Polyphenol-Enriched Fractions of C. subternata

Several factors determine the adsorption capacity of a system so that it cannot be predicted. These factors are the characteristics of both the adsorbent (e.g., surface area and particle size) and the adsorbate (e.g., structure, water solubility, polarity, size, and molecular weight), as well as that of the solvent (e.g., polarity, pH, and temperature) [11]. Therefore, static and dynamic adsorption experiments were used to determine the most suitable experimental conditions to produce polyphenol-enriched fractions from a hot water extract of *C. subternata*. The static adsorption experiments indicated that the XAD 1180N resin was more suitable than the HP20 resin due to its higher adsorption ratios for some of the target compounds. A sample concentration of 3 mg/mL and a contact time of 90 min were required to obtain good adsorption of these phenolic compounds onto the resin. The desorption profile of the compounds indicated that a step-wise gradient from 12–50% EtOH should be suitable.

Although the static experiments provided information on the effectiveness of the adsorbent, the results are not directly transferable to a column system [11] and subsequently, dynamic adsorption and desorption studies were conducted using a fixed-bed column for scalability. In dynamic adsorption, column loading is performed until the concentration of the target compound in the eluate exceeds a predefined threshold level (%) referred to as the breakthrough point [19]. This breakthrough percentage value is defined by the user, and reported values ranged from 3% [13] to 10% [20], depending on the purpose of the separation. In the present study, the maximum sample loading (7 BVs of 10 mg/mL solution; 6.72 g extract) was determined based on a 10% breakthrough value for IDG, the compound with the least affinity for the resin.

The step-wise desorption gradient, consisting of 3 BV each of 12%, 20%, 30% and 50% EtOH, was found suitable for crude fractionation of the extract into four fractions enriched in different phenolic compounds. Linear upscaling of the fractionation column (22 times) was very successful as also previously reported by Miller et al. [13] for a *C. genistoides* extract. Linear scalability plays a key role in the development of industrial-scale processes [21]. Besides the column height-to-diameter ratio, other factors such as pressure drop, the compressibility of the resin and wall friction also need to be considered in such a case [22]. The phenolic compounds in the four fractions were identified by comparing their UV-vis spectral data, accurate mass and MS fragmentation patterns to data previously reported in the literature [7,23–25]. The main phenolic compounds of the respective fractions were IDG and IMG (fraction 1), mangiferin, isomangiferin, HPDG and vicenin-2 (fraction 2), PDG, eriocitrin and scolymoside (fraction 3) and hesperidin and *p*-coumaric acid (fraction 4).

4.2. Bioactivity of C. subternata Extract and Fractions

The differences in bioactivity between the extract and fractions provided some insight into the compounds responsible for the bioactivity. Fraction 4 enriched in hesperidin was less effective than the extract in scavenging $O_2^{\bullet -}$. Orallo et al. [26] reported that

hesperidin showed no $O_2^{\bullet -}$ scavenging activity even at 100 µM. Scavenging of DPPH$^\bullet$ was less selective since only fraction 1, enriched in IDG and IMG, was less effective than the extract, confirming previous results that both are comparatively weak DPPH$^\bullet$ scavengers [27,28]. Their weak activity could be attributed to the replacement of the C-7 OH-group with a glucopyranosyl moiety, which sterically prevents the remaining free OH-groups from accessing the radical site [29]. The high activity of fraction 2 is attributed to its high mangiferin and isomangiferin content. Both compounds are well-known radical scavengers [28,30]. DPPH$^\bullet$ scavenging activity of fraction 3 is attributed to its high PDG content. The free hydroxyl groups at the 2′ and 6′ positions of the A ring of the dihydrochalcone are essential for effective radical scavenging activity [31,32]. The major phenolic compound in fraction 4, namely hesperidin, is also known for good DPPH$^\bullet$ scavenging activity [33].

The *C. subternata* extract and fractions showed poor XO inhibitory activity ($\leq$40% at 500 µg/mL). According to previous studies, a planar flavonoid structure created by the double bond between C-2 and C-3 is required for strong XO inhibitory action [34,35]. A large complement of *C. subternata* flavonoids, however, lacks this double bond, explaining the relatively low inhibitory activity. Furthermore, free hydroxyl groups at C-5 and C-7 are also deemed essential for XO inhibition [36,37]. Whilst vicenin-2, a flavone, fulfills all these criteria, only small amounts are present in the extract and fractions.

Only the extract and fraction 1 inhibited IgE-mediated degranulation of RBL-2H3 cells to some extent, but fractionation did not improve this activity despite enrichment in specific polyphenols. This is contrary to what would be expected as many polyphenols, especially planar flavonoids such as flavones and flavonols, have shown activity in this model [12]. Glycosylation had a severe negative effect on the activity of flavones and flavonols in the study by Mastuda et al. [12]. However, Suntivich et al. [38] showed ca. 50% inhibition of mast cell degranulation for the glycosylated flavone luteoloside at 25 µM. This is relevant for the planar flavone glycosides, vicenin-2 and scolymoside, in fractions 2 and 3, respectively. Flavanones were shown to have poor activity [12] as observed for fraction 4, enriched in hesperidin. It is thus likely that IDG and IMG (both glycosides) will also not be effective inhibitors of IgE-mediated degranulation of RBL-2H3 cells. Further investigation of fraction 1 is needed to identify active compounds.

Despite no information on their activity in the RBL-2H3 cell model, mangiferin [39], hesperidin [40], scolymoside [41] and vicenin-2 [41] have all demonstrated anti-inflammatory and/or anti-allergic properties in other models. Nothofagin (3′-D-glucopyranosylphloretin), related to the *C. subternata* dihydrochalcone, PDG, suppresses mast cell-mediated allergic inflammation [42]. Together with these reports and our previous study, *C. subternata* extracts might include several anti-allergic substances with different mechanisms such as regulatory T cell induction, Th2 suppression, and anti-degranulation.

The relative activity of the extract and fractions in the different assays demonstrated that radical scavenging, irrespective of the radical, is not a good proxy for inhibition of mast cell degranulation, despite the similar structural features of flavonoids that determine both types of activity [12,43].

5. Conclusions

A MARC protocol for fractionation of a *C. subternata* hot water extract was successfully developed and implemented to obtain four fractions with differing phenolic compositions. Despite enrichment of the fractions in specific polyphenols and the increased DPPH$^\bullet$, ORAC and XO inhibitory activity of some fractions, the inhibition of mast cell degranulation by the extract was only slightly enhanced by fractionation. The antioxidant and XO inhibitory assays were, therefore, not good proxies for screening the anti-allergy potential of *C. subternata* extract and fractions, despite the similar structural features of flavonoids that determine both types of activity. Fraction 1 exhibited anti-allergy potential and needs to be further investigated to determine the compounds responsible for the activity.

Supplementary Materials: The following supporting information can be downloaded at: https://www.mdpi.com/article/10.3390/separations9100278/s1, Table S1: Adsorption capacity (mg/g) of XAD 1180N and HP20 macroporous resins for *Cyclopia subternata* phenolic compounds as a function of sample concentration (mg/mL); Table S2: Adsorption ratios (%) for *Cyclopia subternata* phenolic compounds on XAD 1180N and HP20 macroporous resins as a function of sample concentration (mg/mL); Table S3: Phenolic compounds identified in a green *Cyclopia subternata* hot water extract and four enriched fractions using high-resolution mass spectrometry in the negative ionization mode; Figure S1: Adsorption ratios of 3-β-D-glucopyranosyl-4-*O*-β-D-glucopyranosyliriflophenone (IDG), 3-β-D-glucopyranosyliriflophenone (IMG) and mangiferin (a) and isomangiferin, vicenin-2 and *p*-coumaric acid (b) on XAD 1180N macroporous resin as a function of contact time (min), using static adsorption; Figure S2: HPLC-DAD chromatograms of a green *Cyclopia subternata* hot water extract (a) and fractions 1–4 (b–e) obtained from large-scale fractionation on XAD 1180N. Peak labels correspond to Table S3.

Author Contributions: C.D.: Investigation, Visualization; H.S.: Investigation; K.O.: Investigation; N.M.: Supervision, Writing—Review & Editing; E.J.: Supervision, Conceptualization, Funding Acquisition, Writing—Original Draft; T.Y.: Conceptualization, Funding Acquisition, Writing—Original Draft; D.d.B.: Conceptualization, Supervision, Writing—Original Draft. All authors have read and agreed to the published version of the manuscript.

Funding: This work was supported by the National Research Foundation of South Africa (NRF grant 131587 to E.J.) and the Department of Science and Innovation (DST/CON 00029/2019; Master's scholarship to C.D.).

Data Availability Statement: The data presented in this study are available in figures and tables, as well as the Supplementary Material.

Conflicts of Interest: The authors declare no conflict of interest.

References

1. Bessa, C.; Francisco, T.; Dias, R.; Mateus, N.; de Freitas, V.; Pérez-Gregorio, R. Use of Polyphenols as Modulators of Food Allergies. From Chemistry to Biological Implications. *Front. Sustain. Food Syst.* **2021**, *5*, 623611. [CrossRef]
2. Loh, W.; Tang, M.L.K. The Epidemiology of Food Allergy in the Global Context. *Int. J. Environ. Res. Public Health* **2018**, *15*, 2043. [CrossRef] [PubMed]
3. Wang, J.; Liu, A.H. Food Allergies and Asthma. *Curr. Opin. Allergy Clin. Immunol.* **2011**, *11*, 249–254. [CrossRef]
4. Singh, A.; Holvoet, S.; Mercenier, A. Dietary Polyphenols in the Prevention and Treatment of Allergic Diseases: Polyphenols Alleviate Allergic Inflammation. *Clin. Exp. Allergy* **2011**, *41*, 1346–1359. [CrossRef] [PubMed]
5. Hosoki, K.; Gandhe, R.; Boldogh, I.; Sur, S. Reactive Oxygen Species (ROS) and Allergic Responses. In *Systems Biology of Free Radicals and Antioxidants*; Laher, I., Ed.; Springer: Berlin/Heidelberg, Germany, 2014; pp. 3239–3266; ISBN 978-3-642-30018-9.
6. Qu, J.; Li, Y.; Zhong, W.; Gao, P.; Hu, C. Recent Developments in the Role of Reactive Oxygen Species in Allergic Asthma. *J. Thorac. Dis.* **2017**, *9*, E32–E43. [CrossRef] [PubMed]
7. De Beer, D.; Schulze, A.E.; Joubert, E.; De Villiers, A.; Malherbe, C.J.; Stander, M.A. Food Ingredient Extracts of *Cyclopia subternata* (Honeybush): Variation in Phenolic Composition and Antioxidant Capacity. *Molecules* **2012**, *17*, 14602–14624. [CrossRef] [PubMed]
8. Murakami, S.; Miura, Y.; Hattori, M.; Matsuda, H.; Malherbe, C.J.; Muller, C.J.F.; Joubert, E.; Yoshida, T. *Cyclopia* Extracts Enhance Th1-, Th2-, and Th17-type T Cell Responses and Induce Foxp3^{+} Cells in Murine Cell Culture. *Planta Med.* **2018**, *84*, 311–319. [CrossRef]
9. Yoshida, T.; Malherbe, C.J.; Okon, K.; Miura, Y.; Hattori, M.; Matsuda, H.; Muller, C.J.; Joubert, E. Enhanced Production of Th1- and Th2-Type Antibodies and Induction of Regulatory T Cells in Mice by Oral Administration of *Cyclopia* Extracts with Similar Phenolic Composition to Honeybush Herbal Tea. *J. Funct. Foods* **2020**, *64*, 103704. [CrossRef]
10. Pérez-Larrán, P.; Díaz-Reinoso, B.; Moure, A.; Alonso, J.L.; Domínguez, H. Adsorption Technologies to Recover and Concentrate Food Polyphenols. *Curr. Opin. Food Sci.* **2018**, *23*, 165–172. [CrossRef]
11. Soto, M.L.; Moure, A.; Domínguez, H.; Parajó, J.C. Recovery, Concentration and Purification of Phenolic Compounds by Adsorption: A Review. *J. Food Eng.* **2011**, *105*, 1–27. [CrossRef]
12. Mastuda, H.; Morikawa, T.; Ueda, K.; Managi, H.; Yoshikawa, M. Structural Requirements of Flavonoids for Inhibition of Antigen-Induced Degranulation, TNF-α and IL-4 Production from RBL-2H3 Cells. *Bioorg. Med. Chem.* **2002**, *10*, 3123–3128. [CrossRef]
13. Miller, N.; Malherbe, C.J.; Joubert, E. Xanthone- and Benzophenone-Enriched Nutraceutical: Development of a Scalable Fractionation Process and Effect of Batch-to-Batch Variation of the Raw Material (*Cyclopia genistoides*). *Sep. Purif. Technol.* **2020**, *237*, 116465. [CrossRef]

14. Wang, W.; Ma, C.; Chen, S.; Zhu, S.; Lou, Z.; Wang, H. Preparative Purification of Epigallocatechin-3-Gallate (EGCG) from Tea Polyphenols by Adsorption Column Chromatography. *Chromatographia* **2014**, *77*, 1643–1652. [CrossRef]
15. Chisté, R.C.; Mercadante, A.Z.; Gomes, A.; Fernandes, E.; Lima, J.; Bragagnolo, N. In Vitro Scavenging Capacity of Annatto Seed Extracts Against Reactive Oxygen and Nitrogen Species. *Food Chem.* **2011**, *127*, 419–426. [CrossRef] [PubMed]
16. Arthur, H.; Joubert, E.; De Beer, D.; Malherbe, C.J.; Witthuhn, C. Phenylethanoid Glycosides as Major Antioxidants in *Lippia multiflora* Herbal Infusion and Their Stability During Steam Pasteurisation of Plant Material. *Food Chem.* **2011**, *127*, 581–588. [CrossRef]
17. Huang, D.; Ou, B.; Hampsch-Woodill, M.; Flanagan, J.A.; Prior, R.L. High-Throughput Assay of Oxygen Radical Absorbance Capacity (ORAC) Using a Multichannel Liquid Handling System Coupled with a Microplate Fluorescence Reader in 96-Well Format. *J. Agric. Food Chem.* **2002**, *50*, 4437–4444. [CrossRef] [PubMed]
18. Leiro, J.M.; Álvarez, E.; Arranz, J.A.; Siso, I.G.; Orallo, F. In Vitro Effects of Mangiferin on Superoxide Concentrations and Expression of the Inducible Nitric Oxide Synthase, Tumour Necrosis Factor-α and Transforming Growth Factor-β Genes. *Biochem. Pharmacol.* **2003**, *65*, 1361–1371. [CrossRef]
19. Kammerer, J.; Carle, R.; Kammerer, D.R. Adsorption and Ion Exchange: Basic Principles and Their Application in Food Processing. *J. Agric. Food Chem.* **2011**, *59*, 22–42. [CrossRef]
20. Soto, M.L.; Moure, A.; Domínguez, H.; Parajó, J.C. Batch and Fixed Bed Column Studies on Phenolic Adsorption from Wine Vinasses by Polymeric Resins. *J. Food Eng.* **2017**, *209*, 52–60. [CrossRef]
21. Putnik, G.; Sluga, A.; ElMaraghy, H.; Teti, R.; Koren, Y.; Tolio, T.; Hon, B. Scalability in Manufacturing Systems Design and Operation: State-of-the-Art and Future Developments Roadmap. *CIRP Ann.* **2013**, *62*, 751–774. [CrossRef]
22. Prentice, J.; Evans, S.T.; Robbins, D.; Ferreira, G. Pressure-Flow Experiments, Packing, and Modeling for Scale-Up of a Mixed Mode Chromatography Column for Biopharmaceutical Manufacturing. *J. Chromatogr. A* **2020**, *1625*, 461117. [CrossRef] [PubMed]
23. Beelders, T.; De Beer, D.; Stander, M.A.; Joubert, E. Comprehensive Phenolic Profiling of *Cyclopia genistoides* (L.) Vent. by LC-DAD-MS and -MS/MS Reveals Novel Xanthone and Benzophenone Constituents. *Molecules* **2014**, *19*, 11760–11790. [CrossRef]
24. Schulze, A.E.; Beelders, T.; Koch, I.S.; Erasmus, L.M.; De Beer, D.; Joubert, E. Honeybush Herbal Teas (*Cyclopia* spp.) Contribute to High Levels of Dietary Exposure to Xanthones, Benzophenones, Dihydrochalcones and Other Bioactive Phenolics. *J. Food Compos. Anal.* **2015**, *44*, 139–148. [CrossRef]
25. Stander, M.A.; Redelinghuys, H.; Masike, K.; Long, H.; Van Wyk, B.-E. Patterns of Variation and Chemosystematic Significance of Phenolic Compounds in the Genus *Cyclopia* (Fabaceae, Podalyrieae). *Molecules* **2019**, *24*, 2352. [CrossRef] [PubMed]
26. Orallo, F.; Álvarez, E.; Basaran, H.; Lugnier, C. Comparative Study of the Vasorelaxant Activity, Superoxide-Scavenging Ability and Cyclic Nucleotide Phosphodiesterase-Inhibitory Effects of Hesperetin and Hesperidin. *Naunyn-Schmiedebergs Arch. Pharmacol.* **2004**, *370*, 452–463. [CrossRef]
27. Malherbe, C.J.; Willenburg, E.; de Beer, D.; Bonnet, S.L.; van der Westhuizen, J.H.; Joubert, E. Iriflophenone-3-*C*-Glucoside From *Cyclopia genistoides*: Isolation and Quantitative Comparison of Antioxidant Capacity with Mangiferin and Isomangiferin Using On-Line HPLC Antioxidant Assays. *J. Chromatogr. B* **2014**, *951–952*, 164–171. [CrossRef]
28. Beelders, T.; de Beer, D.; Joubert, E. Thermal Degradation Kinetics Modeling of Benzophenones and Xanthones during High-Temperature Oxidation of *Cyclopia genistoides* (L.) Vent. Plant Material. *J. Agric. Food Chem.* **2015**, *63*, 5518–5527. [CrossRef]
29. Xie, J.; Schaich, K.M. Re-Evaluation of the 2,2-Diphenyl-1-Picrylhydrazyl Free Radical (DPPH) Assay for Antioxidant Activity. *J. Agric. Food Chem.* **2014**, *62*, 4251–4260. [CrossRef]
30. Vyas, A.; Syeda, K.; Ahmad, A.; Padhye, S.; Sarkar, F.H. Perspectives on Medicinal Properties of Mangiferin. *Mini-Rev. Med. Chem.* **2012**, *12*, 412–425. [CrossRef]
31. Rezk, B.M.; Haenen, G.; van der Vijgh, W.J.; Bast, A. The Antioxidant Activity of Phloretin: The Disclosure of a New Antioxidant Pharmacophore in Flavonoids. *Biochem. Biophys. Res. Commun.* **2002**, *295*, 9–13. [CrossRef]
32. Nakamura, Y.; Watanabe, S.; Miyake, N.; Kohno, A.H.; Osawa, T. Dihydrochalcones: Evaluation as Novel Radical Scavenging Antioxidants. *J. Agric. Food Chem.* **2003**, *51*, 3309–3312. [CrossRef] [PubMed]
33. Wilmsen, P.K.; Spada, D.S.; Salvador, M. Antioxidant Activity of the Flavonoid Hesperidin in Chemical and Biological Systems. *J. Agric. Food Chem.* **2005**, *53*, 4757–4761. [CrossRef] [PubMed]
34. Cos, P.; Ying, L.; Calomme, M.; Hu, J.P.; Cimanga, K.; Van Poel, B.; Pieters, L.; Vlietinck, A.A.J.; Berghe, D.V. Structure−Activity Relationship and Classification of Flavonoids as Inhibitors of Xanthine Oxidase and Superoxide Scavengers. *J. Nat. Prod.* **1998**, *61*, 71–76. [CrossRef] [PubMed]
35. Nagao, A.; Seki, M.; Kobayashi, H. Inhibition of Xanthine Oxidase by Flavonoids. *Biosci. Biotechnol. Biochem.* **1999**, *63*, 1787–1790. [CrossRef]
36. Da Silva, S.L.; Da Silva, A.; Honório, K.M.; Marangoni, S.; Toyama, M.H.; Da Silva, A.B.F. The Influence of Electronic, Steric and Hydrophobic Properties of Flavonoid Compounds in the Inhibition of the Xanthine Oxidase. *J. Mol. Struct. THEOCHEM* **2004**, *684*, 1–7. [CrossRef]
37. Van Hoorn, D.E.C.; Nijveldt, R.J.; Van Leeuwen, P.A.M.; Hofman, Z.; M'Rabet, L.; De Bont, D.B.A.; Van Norren, K. Accurate Prediction of Xanthine Oxidase Inhibition Based on the Structure of Flavonoids. *Eur. J. Pharmacol.* **2002**, *451*, 111–118. [CrossRef]
38. Suntivich, R.; Songjang, W.; Jiraviriyakul, A.; Ruchirawat, S.; Chatwichien, J. LC-MS/MS Metabolomics-Facilitated Identification of the Active Compounds Responsible for Anti-Allergic Activity of the Ethanol Extract of *Xenostegia tridentata*. *PLoS ONE* **2022**, *17*, e0265505. [CrossRef]

39. Piao, C.H.; Fan, Y.J.; Van Nguyen, T.; Song, C.H.; Chai, O.H. Mangiferin Alleviates Ovalbumin-Induced Allergic Rhinitis via Nrf2/HO-1/NF-κB Signaling Pathways. *Int. J. Mol. Sci.* **2020**, *21*, 3415. [CrossRef]
40. Wei, D.; Ci, X.; Chu, X.; Wei, M.; Hua, S.; Deng, X. Hesperidin Suppresses Ovalbumin-Induced Airway Inflammation in a Mouse Allergic Asthma Model. *Inflammation* **2012**, *35*, 114–121. [CrossRef]
41. Kang, H.; Ku, S.-K.; Jung, B.; Bae, J.-S. Anti-Inflammatory Effects of Vicenin-2 and Scolymoside In Vitro and In Vivo. *Agents Actions* **2015**, *64*, 1005–1021. [CrossRef]
42. Kang, B.-C.; Kim, M.-J.; Lee, S.; Choi, Y.-A.; Park, P.-H.; Shin, T.-Y.; Kwon, T.K.; Khang, D.; Kim, S.-H. Nothofagin Suppresses Mast Cell-Mediated Allergic Inflammation. *Chem.-Biol. Interact.* **2019**, *298*, 1–7. [CrossRef] [PubMed]
43. Heim, K.E.; Tagliaferro, A.R.; Bobilya, D.J. Flavonoid Antioxidants: Chemistry, Metabolism and Structure-Activity Relationships. *J. Nutr. Biochem.* **2002**, *13*, 572–584. [CrossRef]